ac-susceptibility measurements on isotropic and anisotropic superconducting networks

M. A. Itzler*
Department of Physics, University of Pennsylvania, Philadelphia, Pennsylvania 19104

G. M. Danner
Department of Physics, Princeton University, Princeton, New Jersey 08544

R. Bojko
National Nanofabrication Facility, Cornell University, Ithaca, New York 14853

P. M. Chaikin
Department of Physics, Princeton University, Princeton, New Jersey 08544
(Received 3 September 1993)

We report measurements of the complex ac susceptibility $\chi(T)$ for both isotropic and anisotropic square superconducting wire networks as well as *direct* measurements of the *magnetic* normal-to-superconducting phase boundary $T_c(H)|_\chi$ for these systems. The $\chi(T)$ transition is substantially broader and exhibits greater depression in magnetic field than the resistive transitions $R(T)$. Commensurability structures found in the $T_c(H)|_\chi$ measurements at low-order rational fields are greatly enhanced compared to those found in resistively measured phase boundaries $T_c(H)|_R$. For square networks made anisotropic by different wire widths in the two perpendicular directions, the $T_c(H)|_\chi$ phase boundaries demonstrate that increasing the anisotropy greatly increases the depression of the susceptibility transition temperature at incommensurate applied magnetic fields. This indicates a weakening of the network's ability to screen magnetic field with larger anisotropy despite the fact that anistropy is increased by *adding* material to one set of parallel wires. This result supports a picture of anisotropic localization of the order parameter and/or anisotropic vanishing of the flux pinning or helicity modulus in periodic systems in an irrational homogeneous field.

I. INTRODUCTION

In the past decade, superconducting networks have proven to be extremely fruitful experimental systems.[1] The behavior of the networks in the presence of a uniform magnetic field can be related to many general problems of current interest in condensed matter physics; these include frustration, commensurability, two-dimensionality phase transitions, localization, and electronic ground states in two-dimensional geometries in perpendicular magnetic fields. As a consequence of fluxoid quantization, the applied magnetic field provides a tunable length scale to complement the length scale already inherent in the network geometry. It is the competition between these two length scales which results in many of the interesting properties of these systems. Furthermore, the description of the superconducting networks by a macroscopic wave function allows the behavior of these systems to be mapped to a mathematically identical problem concerning the states of a single electron on a lattice of the same geometry in a magnetic field. Therefore, studying the networks gives us insight into the nature of these electronic states.

In particular, we have recently reported[2] evidence for the apparent localization of the superconducting order parameter in square networks into which anisotropy was introduced by making one set of parallel wires wider than the perpendicular set. Four-point resistive measurements were used to independently probe the two sets of wires and show that at incommensurate values of the applied field, the resistive T_c [operationally defined as $R(T_c)=\epsilon_R R_n$ with $\epsilon_R \sim 0.3$, as discussed below] along the narrow wires was substantially depressed below T_c measured along the wide wires.

In general, an explanation for the behavior of these network systems is sought using linearized Ginzburg-Landau (LGL) theory as originally applied to networks by de Gennes[3] and Alexander.[4] For the isotropic square network, the solution for the field-dependent transition temperature $T_c(H)$ is formally equivalent to the maximum eigenvalue of the spectrum for a tight-binding electron on a square lattice in a homogeneous applied magnetic field; therefore, the phase boundary for an isotropic square network is just the upper edge of the celebrated Hofstadter Butterfly.[5] A similar solution for the *anisotropic* square network can be found using appropriate modifications to the Hofstadter solution. (Specifically, the complementary electron problem is one in which the tight-binding transfer integrals differ along the two different directions of the square lattice.) We have shown[2] that this solution provides an excellent fit for T_c measured resistively along the wide wires of the anisotropic network. This is reasonable given that the LGL theory yields the highest temperature at which *any* part of the system exhibits a nonzero order parameter. Since we found T_c of the wide wires always equals or exceeds

that of the narrow wires, the LGL result can be expected to describe the wide wire phase boundary. However, the LGL solution provides no explanation for the behavior of the narrow wires.

Additional insight concerning the anisotropic system was provided by Aubry and André[6] in their theoretical treatment of the anisotropic tight-binding bands. They found that for incommensurate magnetic fields, the wave function is anisotropically localized; i.e., it is extended along the strongly coupled direction while being localized along the weakly coupled direction. This is entirely consistent with our experimental results on the anisotropic networks at incommensurate fields: at temperatures for which the wide wires showed a loss of resistive sensitivity (indicating an extended order parameter), the narrow wides retained a large fraction of their normal resistance (indicating localized behavior). Only at much lower temperatures did the narrow wires exhibit a vanishing resistance.

As with all resistive measurements on superconducting networks, the fairly narrow R vs T transition limited the range of temperatures for which these previous experiments were sensitive. In the interest of studying networks (particularly the anisotropic networks) at lower temperatures, we have measured their complex ac susceptibility χ using a mutual inductance technique first employed by Shoenberg.[7] This experimental approach has many advantages including high sensitivity, simplicity of construction, and versatility with regard to sample size and shape. Recently, beautiful measurements have been made on thin films and networks by Hebard and Fiory[8] and by Martinoli's group[9] using a variation of this technique. However, our experimental setup is more similar to that used previously by Pannetier's group.[10]

In the past, we have measured resistive phase boundaries by assuming that T_c corresponds to a temperature at which the network resistance falls to some chosen fraction of its normal resistance R_n. (Although in practice we may choose an arbitrary fraction of R_n, experience has shown that the best agreement with the mean-field solution given by LGL theory is found for values in the range $\sim 30-50\%$ of R_n.) A feedback loop maintained this resistance while the magnetic field was swept by adjusting the temperature of the system. The temperature thus obtained at any field H can then be identified with the critical temperature $T_c(H)|_R$, where $|_R$ indicates that we are using a particular fractional value $\epsilon_R = R(T_c)/R_n$ as our criterion for T_c.

In an analogous way, we have *directly* measured a *magnetic* phase boundary $T_c(H)|_\chi$ by using a fixed value of the susceptibility χ in the $\chi(T)$ transition as our criterion for the "magnetic" transition temperature [i.e., $T_c(H)$ is defined by $\chi(H,T_c) \equiv [(1-\epsilon_\chi)\chi_s + \epsilon_\chi \chi_n]$, where $\chi_n(\chi_s)$ is the normal (superconducting) susceptibility]. Gandit *et al.*[10] previously measured $\chi(H)$ at fixed temperatures for isotropic square nets and indirectly deduced a magnetic phase boundary from those sweeps, but as we shall see, direct measurements of $T_c(H)|_\chi$ reveal much greater detail. For both isotropic and anisotropic square networks, we have found that the structure at commensurate fields is greatly enhanced and is evident out to higher-order fields when compared to similar structures found in the resistively measured phase boundaries $T_c(H)|_R$. Additionally, the $\chi(T)$ transitions are much broader and substantially depressed in temperature relative to the $R(T)$ transitions.

The measurements of $T_c(H)|_\chi$ for the anisotropic networks also reveal the following remarkable behavior. At incommensurate applied fields, the susceptibility transition temperature is greatly depressed as the anisotropy is increased. This transition essentially probes the change in the sample's ability to screen magnetic fields. Therefore, at incommensurate fields, samples with larger anisotropy screen much more *weakly* (i.e., at a given temperature in the transition region) even though the anisotropy is increased by *adding* material to one set of parallel lines (making them wider) while leaving the other set unchanged. This result is consistent with the idea suggested by our earlier resistive measurements[2] that the superconducting order parameter is anisotropically localized as was first predicted in the work of Aubry and André[6] and that the effects of this localization are more pronounced with increasing anisotropy. However, recent theoretical studies of anisotropic networks show complementary effects with presumably related origins. For networks at rational fields Hu and Niu[11] found interesting temperature dependences to the flux lattice structure and "weakened" correlations for flux lines separated by thicker wires. Alternatively, Monte Carlo studies of frustrated XY models with anisotropy show that the rigidity or helicity modulus becomes finite at a higher temperature in one direction than another. This would yield a temperature range in which the flux lines are pinned in one direction but not another. The magnetic screening measured by χ would not be effective until the flux is pinned in all directions.

The remainder of this paper is organized as follows. Section II contains experimental details. In Sec. III, we report the results of susceptibility measurements made on isotropic square networks, and Sec. IV contains the results of similar measurements made on the anisotropic square nets. We discuss these results in Sec. V and present our conclusions in Sec. VI.

II. EXPERIMENTAL DETAILS

The networks studied in these experiments were fabricated at the National Nanofabrication Facility at Cornell University using standard bilevel electron beam lithography. All samples consisted of 500-Å-thick aluminum deposited by e-beam evaporation in a square lattice geometry of 400×400 lines with a 2.0-μm center-to-center line spacing. For the isotropic networks, all lines had a width of 2300 Å. In the anisotropic samples, the narrow set of parallel lines had a 2300-Å linewidth while the wide lines in the perpendicular direction had widths varying from 1 to 4 times that of the narrow lines. Resistivities of simultaneously evaporated solid films were on the order of 1 $\mu\Omega$ cm.

The apparatus for the susceptibility measurements was

based on a mutual inductance technique employing two counterwound pickup coils driven by a single coaxial drive coil (see Fig. 1). For geometrically identical pickups (aside from the winding direction), the net emf across the pair due to the drive field should be zero since they are counterwound. Once the net signal across the pair is nulled with a sample inside one of the pickups, any change in the sample's magnetization will change the inductance of this pickup and generate a signal proportional to the sample's magnetization. By applying a time-varying field dH, the derivative of this magnetization dM/dH can be measured and used to calculate the complex susceptibility $\chi \equiv \chi' + i\chi''$ of the sample. This measurement can be made in the presence of any external dc magnetic field.

The real part of the susceptibility, χ', is essentially a measure of the sample's screening capacity. If the sample's skin depth or penetration depth δ is much greater than its characteristic dimension a, there is practically no screening and $\chi' \sim 0$; conversely, if $\delta \ll a$, then χ' attains its saturation value. Dissipation in the sample is given by the imaginary part χ''. For $\delta \gg a$, there are negligible screening currents and therefore there is negligible dissipation; when $\delta \ll a$, screening currents are carried only at the sample's surface and again the dissipation is small. In the intermediate range $\delta \sim a$, the dissipation (and therefore χ'') reaches its peak value. For a good conductor, the skin depth $\delta \propto 1/\sqrt{\sigma}$ where σ is the intrinsic conductivity of the sample. One can then interpret a finite width normal-to-superconductivity susceptibility transition as the temperature range in which the sample conductivity increases from its normal-state value to the saturation value in the superconducting state (where $\sigma \to \infty$ for $\omega \to 0$). Finite resistivity can result from order-parameter amplitude fluctuations (to zero) or phase fluctuations (motion of flux lines).

Small residual offsets present after cooling the counterwound pickups to helium temperatures were canceled using an ac bridge circuit. Each pickup served as one arm of the bridge, and variable resistance and capacitance on the remaining arms were adjusted to achieve an acceptable null. Both the real and imaginary parts of χ were measured simultaneously using a PAR 5301 dual-phase lock-in amplifier. Generally, the phase was set to give $\chi'' = 0$ when the sample temperature was well below the χ transition (where the dissipation can be expected to be negligible).

As illustrated in Fig. 1, samples were mounted on a single-crystal quartz pedestal so that they were positioned at the center of one pickup where the maximum signal was obtained. Leads for making simultaneous resistive measurements were also present. The apparatus sensitivity was calibrated using a known sinusoidally varying magnetic moment (a small current loop); for the pickups used in most of the measurements, this value was 1.0×10^{-6} esu/μV/kHz. A drive current of 100 μA generated an oscillating drive field $dH \sim 16$ mG; this amplitude was determined to be well within the linear response regime. Drive coils were made with a single layer of approximately 100 turns of 38 AWG copper wire, and the pickups typically had between 1000 and 2000 turns of 44 AWG wire wound in many (~ 50) layers. The large turns ratio (100:2000) was necessary to achieve sufficient sensitivity while using a drive field dH small enough not to perturb the system.

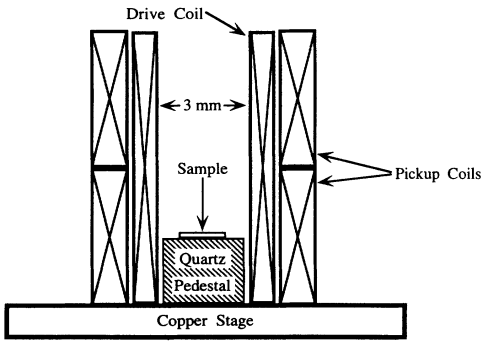

FIG. 1. Schematic diagram of coil setup and sample placement for mutual inductance technique used to measure complex ac susceptibility of superconducting networks. The copper stage is at the end of a cold finger capable of reaching ~ 500 mK.

III. ISOTROPIC NETWORK RESULTS

Before considering the anisotropic samples, we will first present typical results for the susceptibility transitions $\chi(T)$ for an isotropic square network; these are shown in Fig. 2. The real part $\chi'(T)$ (upper part of left-hand vertical scale) and the imaginary part $\chi''(T)$ (lower part of left-hand scale) are plotted with the $R(T)$ resistive transitions (right-hand vertical scale). The rightmost curve of each type is taken at zero field; the middle curves are for $f = \frac{1}{2}$, and the leftmost curves are for $f = 0.618\ldots$, where f is the average flux per unit cell of the square lattice. [The third value corresponds to the irrational field $f = 1/\tau = (\sqrt{5}-1)/2$, the inverse of the

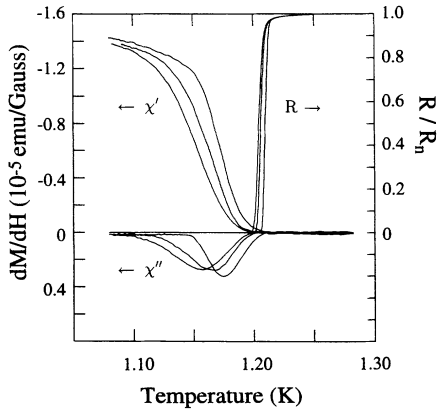

FIG. 2. Susceptibility and resistive transitions for an isotropic square network. $\chi'(T)$ is on upper part of left-hand vertical scale, $\chi''(T)$ is on lower part of left-hand scale, and $R(T)$ is on right-hand vertical scale. The rightmost curve of each type is taken at zero field: the middle curves are for $f = \frac{1}{2}$, and the leftmost curves are for $f = 0.618\ldots$.

golden man.] All three curves at a given field were taken simultaneously. Curves for $f=1$ are not shown since these were identical to the $f=0$ results aside from a slight depression in temperature (a few mK) due to flux expulsion from the bulk of the wires. Perhaps the most obvious feature in Fig. 2 is that the susceptibility transitions are substantially wider than the resistive transitions; whereas zero-field resistive transition widths (10%–90%) are about 3–5 mK, the susceptibility transition widths at zero field are on the order of 40 mK. [The $\chi(T)$ width is taken to be the distance between the two points at which χ'' is 10% of its peak value. This seems to be a more reasonable criterion than any using $\chi'(T)$ since the saturation beyond the knee in $\chi'(T)$ is rather slow.] Another feature is the depression and broadening of both parts of $\chi(T)$ in a magnetic field. The depression is much greater at the incommensurate field $f=0.618\ldots$ than it is at the commensurate filed $f=\frac{1}{2}$. The incommensurate case also shows somewhat larger broadening. A third characteristic of these transitions is that the onset of the $\chi(T)$ transition clearly overlaps the resistive transition tail at all field values. [This is seen most obviously where the $\chi'(T)$ curves cross the tails of the $R(T)$ transitions near 1.20 K.]

The $\chi(T)$ measurements were made at frequencies ranging from 1 to 50 kHz. In this range, we found no frequency dependence for these transitions to within an uncertainty of ±5 mK. This indicates that there is no distinct Kosterlitz-Thouless transition in these systems; if the $\chi(T)$ transition were KT-like, it would exhibit a noticeable frequency dependence.[8] This conclusion is consistent with the fact that the small network resistances render the KT transition temperature T_{KT} indistinguishable from the mean-field T_c since the difference T_c-T_{KT} is expected to be much smaller than the measured mean-field transition width of 3–5 mK.

Using the calibration from the previous section, we can calculate the susceptibility and demagnetization factor for the samples from the saturation value of dM/dH. Since the samples are thin films, we can expect the demagnetization factor η [given by $\chi=-1/4\pi(1-\eta)$] to be quite close to 1 and χ to therefore be quite large. Typical saturation values for dM/dH were about 1.5×10^{-5} esu cm/G (see Fig. 2), and sample volumes were about $(0.82\text{ nm})^2\times0.05\ \mu\text{m}=3.36\times10^{-5}\ \text{cm}^3$. (In calculating the volume, we treat the networks as continuous films. This seems appropriate since solid films did, in fact, have the same saturation value.) Therefore, the measured volume susceptibility $\chi_v=(1/V)(dM/dH)$ is about -450. This is much larger than the value $-1/(4\pi)$ expected for bulk superconductors (at least when $\eta\sim0$) because the film excludes flux from a roughly spherical volume with a diameter equivalent to the linear dimension of the film. These results are consistent with values reported by Gandit *et al.* [10] for square indium networks which were 6 mm on a side. Their value for the volume susceptibility ($\chi_v\sim-3500$) is larger by approximately a factor of the ratio of their linear sample dimension (6 mm) to our linear sample dimension (0.82 mm). It is clear that this should be the case when one considers that although their sample volume is larger by this ratio *squared,* their screening volume is larger by this ratio *cubed.* Therefore, their value for χ_v should be larger by a single power of this ratio.

In an attempt to account for the zero-field width of the $\chi(T)$ transition, χ can be viewed as a contactless measurement of the complex impedance of the sample with greater sensitivity than that of the resistive measurement. We expect that the peak in the dissipative part $\chi''(T)$ will occur when the magnetic penetration depth is on the order of the sample size. We start with Pearl's form[12] for the penetration depth in the two-dimensional limit: $\Lambda=2\lambda^2/d$, where λ is the bulk penetration depth and d the sample thickness. The temperature dependence for λ is[13] $\lambda=\lambda_{\text{eff}}(0)[(T_c-T)/T_c]^{-1/2}$, where $\lambda_{\text{eff}}(0)=\lambda_0^{\text{clean}}(\xi_0/1.33l)^{1/2}$ is the zero-temperature penetration depth in the dirty limit; in aluminum, $\lambda_0^{\text{clean}}=0.016\ \mu$m, $\xi_0\sim1.6\ \mu$m, and the sample mean free path $l\sim0.0235\ \mu$m as determined elsewhere.[14] Finally, we must consider that the square lattice is mostly devoid of material thereby reducing its screening ability, and we should correct for this by dividing by the linear filling factor of $\sim\frac{1}{8}$ (assuming line widths of $\sim0.25\ \mu$m and lattice constants of 2 μm). This gives a difference between the resistive T_c and the temperature at the peak in $\chi''(T)$ of $\Delta T_c\sim5.3$ mK which is off by a factor of 6 from the measured value of ~30 mK. Therefore, the above analysis is insufficient to account for the $\chi(T)$ transition widths. (However, the small filling factor in the isotropic networks does make an unambiguous contribution to the width since solid thin films were found to have a dissipation peak at a substantially smaller value of $\Delta T_c\sim10$ mK.)

As described in the introductory section above, we can measure a magnetic phase boundary $T_c(H)|_\chi$ by fixing χ at some fraction of its maximum value using a feedback loop while the field H is swept. Locking into either χ' or χ'' gives qualitatively similar results, and so the data shown below were taken using a fixed value only in the χ' transition. Results were also fairly insensitive to the precise lock-in value as long as it was not too close to the transition tails. Figure 3 shows $T_c(H)|_\chi$, where χ' was fixed at 50% of its saturation value ($\epsilon_\chi=0.5$), and the lower curve is the resistive phase boundary $T_c(H)|_R$ (with $\epsilon_R\sim0.3$) for the same sample. The magnetic phase boundary shows much larger commensurability structure, and this structure is apparent for higher-order commensurate states: structures at $f=\frac{1}{6}$ are fairly unambiguous on the magnetic phase boundary whereas structure at $f=\frac{1}{4}$ on the resistive phase boundary is completely absent. In fact, the magnetic $T_c(H)$ bears a closer resemblance to Josephson junction array data;[1] this is perhaps not so surprising given that the susceptibility data are taken well below the GL transition temperature so that we are no longer in the mean-field regime.

In the presence of a finite magnetic field the ac penetration depth depends on flux pinning and dissipation. The interpretation of the susceptibility in this picture is that the harmonic pinning constants are large for low-order commensurate states and progressively smaller for less commensurate states. The finite pinning for incommensurate states presumably comes from imperfections.

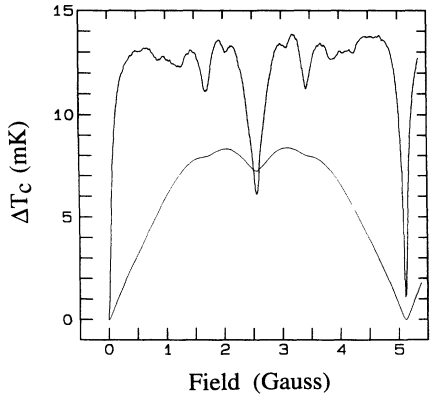

FIG. 3. Magnetic phase boundary $T_c(H)|_\chi$ of an isotropic square network taken by locking into 50% of the saturation value in the $\chi'(T)$ transition. The lower curve (thin line) is the resistive phase boundary $T_c(H)|_R$ of the same sample. $T_c(H)|_\chi$ shows much larger commensurability structure which is apparent for higher-order commensurate fields.

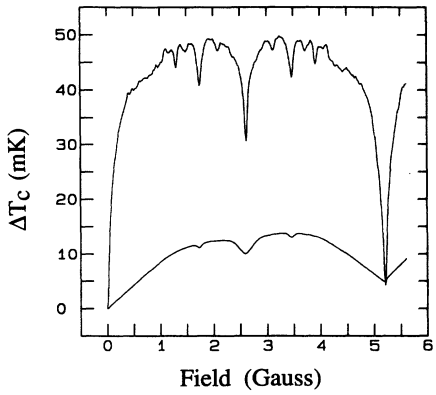

FIG. 5. Magnetic phase boundary $T_c(H)|_\chi$ of an anisotropic square network taken by locking into 30% of the saturation value in the $\chi'(T)$ transition. The lower curve (thin line) is the resistive phase boundary $T_c(H)|_R$ of the same sample. As in the case of the isotropic sample, $T_c(H)|_\chi$ shows much larger commensurability structure which is apparent for higher-order commensurate fields. However, the depression of $T_c(H)|_\chi$ for the anisotropic case at incommensurate fields is much more pronounced.

Since the pinning constants increase with lower temperatures, the $T_c(H)|_\chi$ measurement then reflects the fact that to get the same pinning (same χ), a lower temperature is required for less commensurate states.

IV. ANISOTROPIC NETWORK RESULTS

The $\chi'(T)$, $\chi''(T)$, and $R(T)$ transitions for an anisotropic network with anisotropy ratio 4:1 are shown in Fig. 4. These curves are presented just as they were in the isotropic case: the rightmost curve of each type is for $f=0$, the middle curve for $f=\frac{1}{2}$, and the leftmost curve is for $f=0.618\ldots$. There are a number of obvious differences from the isotropic network data. First, the zero-field width of $\chi(T)$ is considerably smaller in this case ($\sim$25 mK). Since the samples are made anisotropic by *adding* material to one set of parallel wires, we might expect that the screening capability of these networks should lie between that of the isotropic samples (zero-field width $\sim$40 mK) and the solid films (zero-field width $\sim$10 mK) as previously discussed. Second, while the broadening of the transitions in field is similar to that of the isotropic samples, the depression of the entire transition is much more pronounced. Third, we find that, at commensurate fields ($f=0$ and $f=\frac{1}{2}$), the onset of $\chi(T)$ occurs just below the resistive transition as it did for the isotropic networks, but at an incommensurate field (e.g., $f=0.618\ldots$) the onset of $\chi(T)$ is pushed down to lower temperatures.

Figure 5 contains the magnetic phase boundary $T_c(H)|_\chi$ for a 3:1 anisotropic sample locked at 30% of

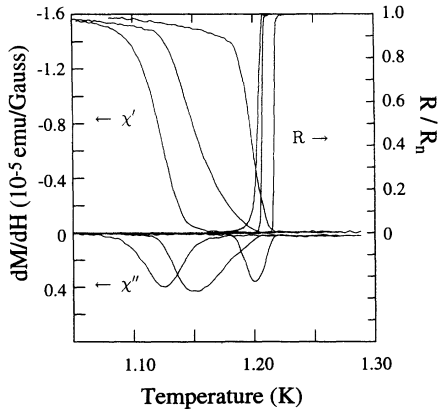

FIG. 4. Susceptibility and resistive transitions for an anisotropic square network. $\chi'(T)$ is on upper part of left-hand vertical scale. $\chi''(T)$ is on lower part of left-hand scale, and $R(T)$ is on right-hand vertical scale. The rightmost curve of each type is taken at zero field; the middle curves are for $f=\frac{1}{2}$, and the leftmost curves are for $f=0.618\ldots$.

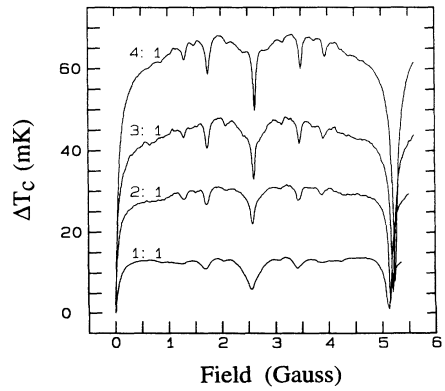

FIG. 6. Magnetic phase boundary $T_c(H)|_\chi$ of anisotropic square networks for anisotropy ratios of (lower to upper): 1:1, 2:1, 3:1, and 4:1. These were taken by locking into 50% of the saturation value in the $\chi'(T)$ transition.

the χ' saturation value. Plotted below this on the same scale is the resistive phase boundary $T_c(H)|_R$ taken by probing the narrow wires for the same sample. As in the isotropic sample data, the magnetic phase boundary shows much deeper structure out to higher-order commensurate fields than the resistive data, and in this case it is even "spikier" than the isotropic sample data. Furthermore, for this case the depression at incommensurate fields is enormous (~ 50 mK).

We can see the dependence of this depression on anisotropy in Fig. 6. In this figure, we present the magnetic phase boundaries $T_c(H)|_\chi$ with χ' locked at 50% for four anisotropy ratios (bottom to top): the isotropic case (1:1), 2:1, 3:1, and 4:1. For larger anisotropy, the increased depression at incommensurate fields is obvious and the structure at commensurate fields grows sharper as well.

V. DISCUSSION

In a previous study[2] we reported the measurement of the resistive transitions for some of these networks. They showed that the resistance along the wide wires is reduced much more rapidly with decreasing temperature than the resistance along the narrow wires, but that this is only true for irrational fields. The present measurement of χ requires circulating screening currents and therefore probes both directions. However, based on resistance measurements presented here and in our earlier work, we expect that the large suppression of the screening response is dominated by the inability of the narrow wires to support supercurrents at the same temperature where such transport is possible along the wide wires. Screening is only effective when the skin depth is comparable to or less than the size of the sample and at our measurement frequency this requires much lower resistances than we can probe with our conventional four-probe technique. The ac susceptibility therefore provides us with a probe much deeper into the superconducting state than resistivity. Once the skin depth calculated from the low-frequency resistivity is less than the sample dimension, the ac screening may still remain small due to weak pinning and a large superconducting penetration depth.

There are two mechanisms which can produce resistance in the vicinity of the superconducting transition in a magnetic field: the magnitude of the order parameter may be zero somewhere in the system yielding a region of normal resistance, or the flux lines piercing the system may not be pinned. The magnitude effects are presumably responsible for the difference between the measured and calculated transition temperatures for disordered networks where it is known that the highest transition temperature state is localized. A more mundane example would be a multilayer sandwich of superconducting and magnetic films which would have resistance at zero temperature. Flux motion corresponds to time-dependent phase slips causing a voltage and resistance. Examples of resistance from flux-line motion are particularly popular in the high-T_c superconductors where the resistive transition is tremendously broadened in the presence of a magnetic field piercing the two-dimensional layers.

In terms of the amplitude effects, a natural explanation of our results can be found in the work of Aubry and André. They showed that the solution to Schrödinger's equation for an electron is an anisotropic tight-binding band in an irrational magnetic field is localized states in the smaller bandwidth direction and extended wave functions in the larger bandwidth direction. For linearized Ginzburg-Landau theory applied to our system, this maps to an extended superconducting order parameter along the wide wires and a localized wave function along the narrow wires. This would naively suggest a zero resistance path along the wide wires and a nonzero path along the narrow wires for the highest-temperature superconducting state. Since the nonlinear problem has not yet been solved, it is not evident how quickly an extended state would develop along the narrow wires as temperature is lowered. The anisotropic extended-localized states may remain considerably more stable energetically to low temperatures. Another scenario is that, on cooling, the order parameter still varies in the weak direction and that these low magnitude strips provide easy pathways for flux motion and phase slip.

The opposite view would be to see what happens when the order parameter is fixed in magnitude at all temperatures, i.e., in a Josephson array or XY model. Recent Monte Carlo techniques allow for the study of incommensurate structures. For commensurate, but fully frustrated fields (one-half flux quanta per cell) in anisotropic triangular XY models the remarkable result was that the rigidity went to zero for directions perpendicular to the strong bonds at lower temperature than along the strong bonds.[15] Moreover, the structure was incommensurate and temperature dependent even though the field itself was commensurate. What this implies for anisotropic Josephson arrays and wire networks without amplitude fluctuations is that the helicity modulus can be zero in one direction and finite in another at a given temperature. This would give finite resistance in one direction (along the weak bonds) and zero in the other (along the strong bonds). It presents the same paradox apparent in the localization problem. If the helicity modulus were to go to zero in one direction while remaining large in the other, the dimensionality would be reduced, and both localization and XY phase transitions are drastically different in one dimension.

Hu and Niu[11] have recently investigated anisotropic square lattices for several rational fields below the superconducting transition. They find the interesting result that the commensurate flux lattice rearranges below T_c and there are several transitions to states with different symmetry. Often the periodicity remains the same perpendicular to the wide wires, but the flux lines move and rearrange in the rows between these wide wires. It appears that there is little interaction between the flux lines in one row and the next. Moreover, the larger the value of q in $f=p/q$, the greater the number of different phases and the more closely spaced are the transition temperatures. This would suggest that for irrational fields (as $q \rightarrow \infty$) the flux lines may have a continuous rearrangement with temperature, a floating incommensurate phase

inside the rows, while they are locked commensurately between rows.

VI. CONCLUSIONS

We have measured the complex susceptibility $\chi(T)$ for both isotropic and anisotropic superconducting square networks. We find that the $\chi(T)$ transitions are substantially broader than the resistive transitions $R(T)$ and occur at lower temperature. We have also reported the first direct measurement of the magnetic phase boundary $T_c(H)|_\chi$ and shown that commensurability structures found in these measurements at low-order rational fields are greatly enhanced compared to those found using resistively measured phase boundaries $T_c(H)|_R$. As far as we know, there is not yet a suitable theoretical description for the magnetic phase boundary which strongly deviates from the mean-field theory phase boundary that has been successfully applied to many resistive transitions. For the anisotropic samples, $T_c(H)|_\chi$ data demonstrate that increasing the sample anisotropy substantially increases the depression of the χ transition temperature at incommensurate fields reflecting a weakening of the network's screening ability even though the anisotropy is enlarged by *adding* material to one set of wires.

The problem of anisotropic superconductivity has gained increased notoriety due to the discovery of the high-temperature superconductors and the even more highly anisotropic organic superconductors. In these systems the motion of flux lines is considerably easier between the planes than for flux piercing the planes or moving across the planes. The present study suggests that the effects of anisotropy and applied field create a situation in which the incommensurability and frustration are concentrated in the "weak" direction and that easy flux motion and low ac screening are the natural consequences. In the anisotropic superconducting networks in irrational magnetic fields, either the order parameter, the helicity modulus, or the flux pinning vanishes in one direction at a lower temperature than in the other.

ACKNOWLEDGMENTS

We would like to acknowledge useful conversations with Chia-Ren Hu, Marc Gabay, and Serge Aubry. Research was supported by the National Science Foundation under Grant No. DMR 92-04581.

---

*Present address: Department of Physics, Harvard University, Cambridge, Massachusetts 02138.

[1]For a comprehensive review of recent work on superconducting networks, see Physica B **152**, 1 (1988).

[2]M. A. Itzler, R. Bojko, and P. M. Chaikin, Europhys. Lett. **20**, 639 (1992).

[3]P. G. de Gennes, C. R. Acad. Sci. Ser. B **292**, 9 (1981); **292**, 279 (1981).

[4]S. Alexander, Phys. Rev. B **27**, 1541 (1983).

[5]Douglas R. Hofstadter, Phys. Rev. B **14**, 2239 (1976).

[6]S. Aubry and C. André, Ann. Israel Phys. Soc. **3**, 133 (1980).

[7]D. Shoenberg, Cambridge Philos. Soc. Proc. **33**, 559 (1937).

[8]A. F. Hebard and A. T. Fiory, Phys. Rev. Lett. **44**, 291 (1980); A. T. Fiory and A. F. Hebard, *Inhomogeneous Superconductors-1979 (Berkeley Springers, WV)*, Proceedings of the Conference on Inhomogeneous Superconductors, AIP Conf. Proc. No. 58, edited by D. U. Gubser, T. L. Francavilla, S. A. Wolf, and J. R. Leibowitz (AIP, New York, 1979).

[9]For a detailed explanation of the mutual inductance technique and references to earlier work, see B. Jeanneret, J. L. Gavilano, G. A. Racine, Ch. Leeman, and P. Martinoli, Appl. Phys. Lett. **55**, 27 (1989).

[10]P. Gandit, J. Chaussy, B. Pannetier, A. Vareille, and A. Tissier, Europhys. Lett. **3**, 623 (1987); P. Gandit, J. Chaussy, B. Pannetier, and R. Rammal, Physica B **152**, 32 (1988).

[11]Chia-Ren Hu and Ming Niu, Bull. Am. Phys. Soc. **38**, 803 (1993); (unpublished).

[12]J. Pearl, Appl. Phys. Lett. **5**, 65 (1964).

[13]See, e.g., M. Tinkham, *Introduction to Superconductivity* (McGraw-Hill, New York, 1975).

[14]M. A. Itzler, Ph.D. dissertation, University of Pennsylvania (unpublished).

[15]W. M. Saslow, M. Gabay, and W.-M. Zhang, Phys. Rev. Lett. **68**, 3627 (1992).